Influence of Shot Peening on the Residual Stresses in Spring Steel Plate

A.T. DeLitizia

Wheelabrator-Frye, A Signal Company
Mishawaka, Indiana, U.S.A.

ABSTRACT

The influence of six different SAE cast steel shot sizes (S-280, S-330, S-390, S-460, S-550, and S-660), measured under constant flow rate of 454 kilograms per minute and the travel speed of the work piece through the blast adjusted to obtain 98 percent coverage in one pass are reviewed as to their induced residual stresses on SAE 5160 leaf spring coupons.

Ten coupons were shot peened with each shot size in the intensity range of 5C to 14C. Random coupons were then checked for residual stress by x-ray diffraction analysis to a depth of .350 mm. Curves were then plotted showing residual stress versus depth below the surface for each coupon. A comparison can then be made of coupons for each shot size and shot intensity as to the residual stresses.

The data was then analyzed mathematically to confirm the conclusions inferred by the composite curves. Cubic parabola regression equations are used to closely predict the measured stress value. The regression curves, plotted from the calculated stress values are compared to the measured stress for each coupon.

KEYWORDS

Shot peening; steel; residual stress; x-ray diffraction; regression equations; fatigue.

INTRODUCTION

In the manufacture of suspension leaf springs shot peening is vital for improving their fatigue life. The benefits of shot peening both in free state and pre-stressed conditions are well documented and have been substantially developed. Specifications on leaf spring manufacture now require a compressive residual stress at a specific depth below the surface.

In order to correlate the needed results with shot peening parameters, a study was undertaken whereby shot sizes and their resulting intensities were compared. Through the methods of residual stress measurement by x-ray diffraction, a "fingerprint" of these compressive stresses can be incorporated into the control of the shot peening process. Prediction of results was also investigated by regression equations to arrive at a model whereby mathematical equations can also be incorporated at the early design stages. The experimental results and comparisons with mathematical models were compared on the basis of accuracy and predictability.

EXPERIMENTAL PROCEDURES

1. Material

The materials involved in the experiment were hot-rolled spring steel plate 7 mm thickness, 70 mm width, and 450 mm length. The weight percent of chemical composition is listed in Table 1. Specimens were normalized, machined, austenitized, quenched and tempered to between 44 and 48 Rockwell C. Free height was 33 mm.

TABLE 1 CHEMICAL COMPOSITION (WEIGHT PERCENT)

SAE No.	C	Mn	P	S	Si	Cr
5160	0.56-0.64	0.75-1.00	.035	.040	0.15-0.36	0.70-0.90

2. SHOT PEENING

Material was prestressed to 6,300 Kg/CM^2 (90,000 psi) and shot peened with a centrifugal wheel to 100 percent coverage. Coverage was measured by the polished strip method using a planimeter to quantitatively determine travel speeds. Flow rate was set for a constant 454 Kgs/min. and wheel speed to a constant 2250 r.p.m. For all tests, Almen intensity is shown in Table 2. Shot for all tests met SAE standards J827 and J444a with hardness range of 44 to 50 Rc.

TABLE 2 INTENSITY

S-280	S-330	S-390	S-460	S-550	S-660
5C	6C	7.5C	9C	11.5C	14C

3. X-RAY DIFFRACTION

X-ray diffraction residual stress measurements were made in the longitudinal direction to the springs and in the center of the concave specimens.

Material was removed for subsurface measurement by electro-polishing in a sulphuric - phosphoric - chromic acid electrolyte minimizing possible alteration of the subsurface residual stress distribution as a result of material removal. Readings were taken to a depth of .350 mm.

4. REGRESSION EQUATIONS

The stress was first plotted vs. depth below the surface for each specimen. An initial regression model of the form: $\sigma = a + by + cy^2$ was chosen where σ equals stress, y, the depth below the surface, and a, b, & c are arbitrary constants.

The method used to estimate these arbitrary constants is called the method of least squares. Simply stated, a matrix equation is set up of the form: $y f = \sigma$

The lower upper decomposition method was used in the calculations which is extremely useful for computerized analysis. After several sets of data were analyzed, it was found that a better fit could be obtained by including the depth cubed term in the regression equation. The equation then took the form: $\sigma = a + by + cy^2 + cy^3$.

The regression equations were then developed. Plots from the calculated stress values were then compared to the X-ray diffraction readings. See Figures 1 to 6.

5. CONCLUSIONS

1) The regression equations closely predict the stress values and can be developed to reduce X-ray diffraction measurements.

2) A pattern exists which indicates that stresses are deeper into the part with larger shot sizes and appears to maximize with S-550.

3) The composite curves drawn by the eyeball of average stress method is similar to those using the regression method.

6. TEST RESULTS

Shot Size (MM)	S-280 (1.1)		S-330 (1.32)		S-390 (1.56)		S-468 (1.84)		S-550 (2.2)		S-660 (2.64)	
Stress (-) (MPa) / Depth (MM)	Meas.	Cal.	Meas.	Cal.	Meas.	Cal.	Meas.	Cal.	Meas.	Cal.	Meas.	Cal.
0	580	589	538	540	593	590	573	594	580	614	455	504
.025	738	704	621	628	656	683	704	697	794	731	656	621
.05	794	800	710	704	773	752	800	780	849	828	745	711
.075	856	869	773	766	828	814	849	842	883	897	787	780
.10	904	924	849	821	869	863	876	883	931	952	862	835
.125	952	952	828	869	911	897	918	918	952	988	814	869
.150	938	966	869	904	897	925	945	938	1000	1014	945	890
.175	1021	959	987	925	932	938	966	945	1035	1021	849	897
.200	938	938	904	931	932	945	897	952	1076	1021	856	897
.225	897	897	938	925	966	945	925	952	1014	1007	869	890
.250	856	849	911	904	938	938	938	945	988	994	890	876
.275	731	780	869	869	932	925	959	938	959	973	849	869
.300	718	704	828	814	911	904	1000	938	897	952	938	856
.325	621	621	711	745	876	883	945	938	994	931	862	856
.350	531	524	676	656	849	856	918	912	904	917	856	856

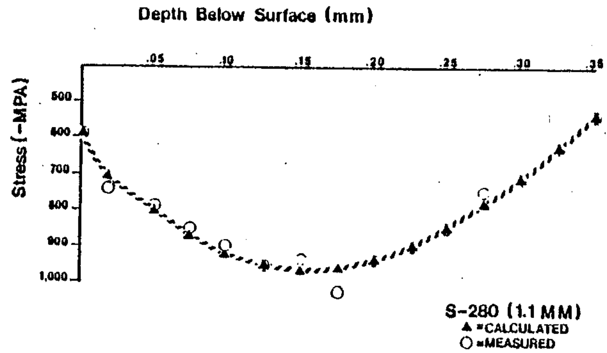

FIG. 1

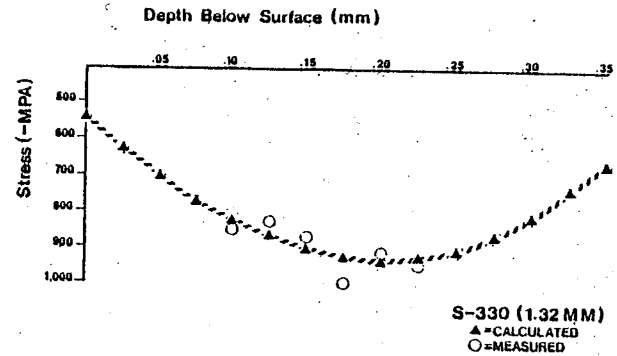

FIG. 2

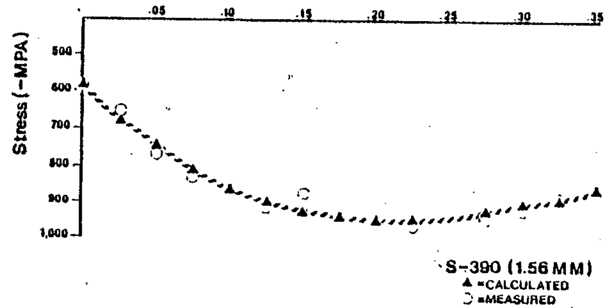

FIG. 3

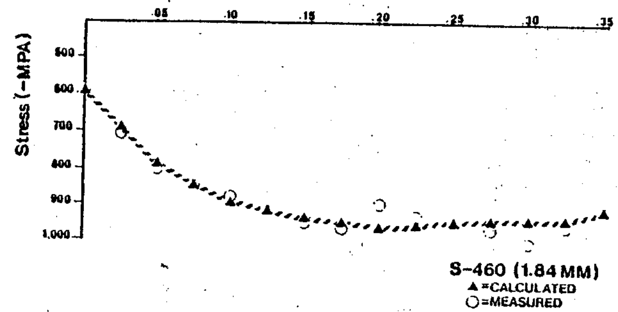

FIG. 4

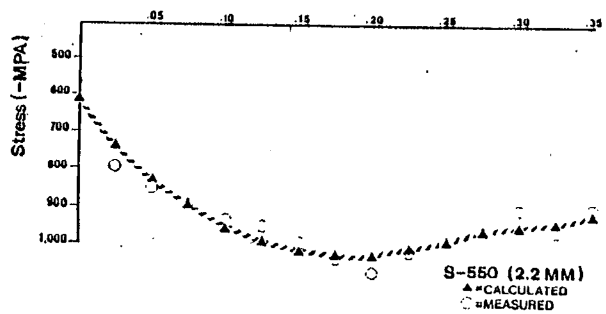

FIG. 5

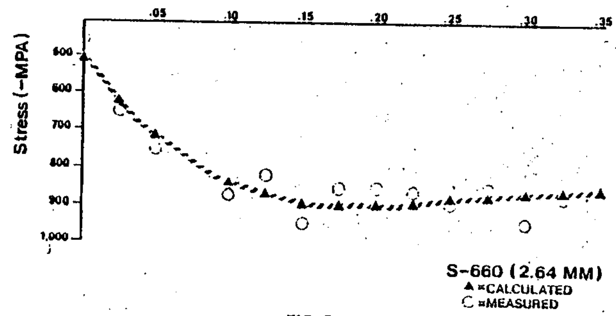

FIG. 6